

Original Research

# Degradation of Atrazine by UV/PMS in Phosphate Buffer

Yixin Lu<sup>1,2</sup>, Zhangkai Ding<sup>2</sup>, Jianqiang Zhang<sup>2\*</sup>, Chenchen Fu<sup>2</sup>,  
Xinyue Xia<sup>2</sup>, Yuxiao Fang<sup>2</sup>

<sup>1</sup>College of Architectural and Environmental Engineering, Chengdu Technological University, Chengdu, China

<sup>2</sup>Faculty of Geosciences and Environmental Engineering, Southwest Jiaotong University, Chengdu, China

Received: 7 June 2018

Accepted: 11 August 2018

## Abstract

The degradation of atrazine (ATZ) by ultraviolet/peroxymonosulfate (UV/PMS) under different conditions was investigated in phosphate buffer, and the degradation mechanism and kinetics were discussed. The results showed that the degradation rate of 2.5  $\mu\text{mol/L}$  ATZ in UV/PMS system was 97.63% in 20 min when the reaction temperature was 20°C, the concentration of PMS was 20  $\mu\text{mol/L}$  and the UV intensity was 50  $\text{mW/cm}^2$  in pH7 phosphate buffer. The mechanism analysis showed that PB with partial alkalinity promoted the degradation of ATZ by UV/PMS more than that with acidic PB. The effect of PB with alkaline conditions on the degradation of ATZ by UV/PMS was more complicated and mainly related to the state of phosphate ions. The UV/PMS system contained both  $\text{HO}\cdot$  and  $\text{SO}_4\cdot^-$ , and the ratio of  $\text{HO}\cdot$ ,  $\text{SO}_4\cdot^-$  and UV-degraded ATZ was nearly 1:1 in pH7 PB. Inorganic anions experiments showed that  $\text{Cl}^-$  and  $\text{HCO}_3^-$  inhibited the degradation of ATZ under UV/PMS, and the inhibitory effect of  $\text{Cl}^-$  was more obvious.  $\text{NO}_3^-$  promoted the degradation of ATZ by UV/PMS. Kinetic analysis showed that UV/PMS degradation of ATZ reaction kinetics was more in line with the quasi first-order reaction kinetics, the inhibition effect of the same concentration of ETA and  $\text{Cl}^-$  on UV/PMS degradation of ATZ are the same, and UV/PMS degradation of ATZ decreased by 38.54% and 36.29% respectively. The addition of  $\text{NO}_3^-$  increased the rate of degradation of ATZ by UV/PMS by 31.21%. By LC-MS analysis, 5 kinds of production m/z and 6 kinds of products were obtained.

**Keywords:** UV/PMS; phosphate buffer; atrazine; kinetics; degradation mechanism

## Introduction

Atrazine, or ATZ, is a pesticide of low cost, good weeding effect and low toxicity [1]. Although ATZ is a low-toxic pesticide, it is difficult to be mineralized

and degraded in the natural environment because of its structural stability in the natural environment [2, 3]. ATZ can be transferred and transformed in different environmental media such as diffusion, volatilization, surface runoff, leaching and both wet and dry deposition. Among these transfers, the methods that ATZ may enter water are mainly surface runoff, leaching and wet and dry deposition [4, 5]. As one of the remaining widely used chemical herbicides, Atrazine

\*e-mail: zhjqicn@swjtu.cn

has been used worldwide for more than 40 years. ATZ and its degradation intermediate products have been detected in the surface water and groundwater of many countries and regions. These chemical substance can cause varying degrees of damage to plants, animals and humans through enrichment of the biological chain [6-9].

ATZ has toxic and endocrine-disrupting detrimental effects on an organism. Research concerning the toxicity effect of ATZ on the freshwater fish *Channa Punctatus* (Bloch) was conducted by Nwani et al. [10], and ATZ with  $LC_{50}$  under 12, 24, 48, 72 and 96 h were measured to be 77.091, 64.053, 49.100, 44.412 and 42.381  $mg \cdot L^{-1}$ , respectively, based on the experimental results. Taveramendoza et al. [11] found that the frequency of primary oogonia occurrence was reduced while the rate of secondary oogonia and atresia showed remarkable increases after exposing stage-56 tadpoles in 21  $\mu g/L$  atrazine for 48 h. According to the studies of Hayes et al. [12, 13], male frogs exposed to water polluted by atrazine with a concentration level above 0.1  $mg/L$  showed a series of symptoms such as hermaphroditism and retarded gonadal development, and the cause was endocrine-disrupting. Besides, the connection between preterm birth and exposure to a commonly used herbicide atrazine in drinking water was studied by Rinsky et al. [14], and the results indicated a greater risk of preterm birth for women in countries with the highest ATZ exposure rate compared with those residing in relatively lower exposure places.

At this point, many advanced oxidation methods based on persulfate have been proved to be effective in degrading ATZ in water. These methods include thermal activation PS [15], Co(II)/PMS [16] and Fe(II)/PS [17] et al. So far, however, there have been few reports about the synergistic degradation of UV/PMS to ATZ. Therefore, this paper will investigate the oxidation degradation effect of UV and PMS to ATZ under different conditions in phosphate buffer and discuss its degradation mechanism and degradation dynamics in order to further enrich chemical pesticide wastewater treatment technology and provide certain reference value.

## Materials and Methods

### Reagents and Instruments

Reagents: Fisher Chemicals, 125555 Sodium Hydroxide, Dodium Dihydrogen Phosphate, Sodium Nitrite, Ethanol, Tert-butanol, Sodium Chloride, Sodium Bicarbonate, Nitrate of Potash – all of which were analytical pure. ATZ and PMS( $KHSO_5 \cdot 0.5KHSO_4 \cdot 0.5K_2SO_4$ ,  $KHSO_5 \geq 47\%$ ) were purchased from Aladdin.

Instruments: 2695-2996 model high-performance liquid chromatograph, electronic scale, Cnlight ZW5D15W-Z150 model UV Lamp, pH meter from

PHSJ-3F Lab in Shanghai Leici, KH5200DB model CNC ultrasonic cleaner, Youpu Ultra-pure Water Purifier, DC-1030 model Energy-saving smart thermostat and 78HW-1 model isothermal magnetism msier.

## Experiment Scheme

### Solution Preparation

The ATZ mother solution was prepared to a concentration of 100  $\mu mol/L$  by ultra-pure water with electrical resistivity of 18.24  $M\Omega \cdot cm$ . The concentration of  $NaH_2PO_4$  solution was prepared to 0.2 mol/L. The concentration of NaOH solution was subdivided into 0.2 mol/L and 0.02 mol/L. The concentration of  $NaNO_2$ , NaCl,  $NaHCO_3$ , and  $KNO_3$  solution was configured to 0.1mol/L, 1mol/L, 0.5mol/L and 1mol/L, respectively. The PMS solution was adjusted to the concentration of 0.01 mol/L and stored out of light. The tert-butyl alcohol solution and ethanol solution was prepared at a concentration of 8 g/L, and preparation methods of pH6, pH7 and pH8 with the constant volume of 1L are shown in Table 1.

### Experiment Scheme of Degradation of ATZ over UV/PMS

To investigate the degradation effect of UV/PMS on ATZ in PB with the concentration of 1.25 mmol/L, the experiments were carried out under different pH values (6, 7 and 8), PMS concentrations (10, 20, 30, 40 and 50  $\mu mol/L$ ), ATZ concentrations (1.25, 2.5, 5  $\mu mol/L$ ) and different UV intensities (30  $mW/cm^2$ , 50  $mW/cm^2$ , 100  $mW/cm^2$ ). Under 20°C water bath, the UV intensity, PB and concentration of PMS and ATZ were respectively 50  $mW/cm^2$ , 1.25 mmol/L, 20  $\mu mol/L$  and 2.5  $\mu mol/L$ . The mechanism of ATZ degradation by different concentrations of tertiary butyl alcohol and ethanol was investigated. The effects of common anion in of  $Cl^-$ ,  $HCO_3^-$  and  $NO_3^-$  in water on the degradation of ATZ over UV/PMS were investigated by adding different concentration solutions of NaCl,  $NaHCO_3$  and  $NaNO_3$ , and the reaction termination agent is  $NaNO_2$  solution with the concentration of 0.1mol/L.

### Analysis Method

The detection of ATZ was conducted by a Symmetry C18 liquid chromatographic column. The specific detection method was as follows: the mobile phase ratio

Table 1. Preparation method for  $NaH_2PO_4$ -NaOH buffer.

pH	0.2 mol/L $NaH_2PO_4$ (mL)	0.2 mol/L NaOH (mL)
6	250	28.50
7	250	148.15
8	250	244.00

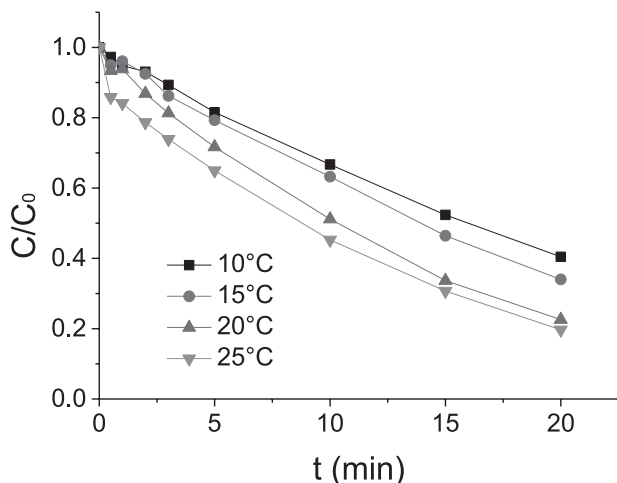


Fig. 1. ATZ removal rate under different temperatures.

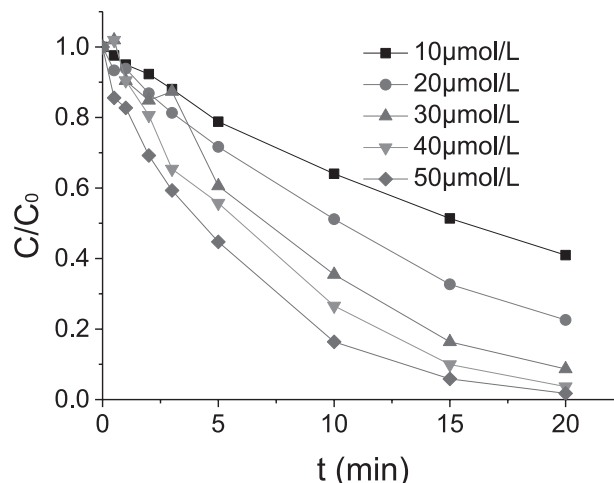


Fig. 2. ATZ removal rates under different PMS densities.

of methyl alcohol accounted for 60% of the solution while ultrapure water accounted for 40%, and the flow velocity, column temperature and determine wavelength were 0.8 mL/min, 40°C and 225nm, respectively. In this study, three parallel tests were conducted for each group of experiments, and the experimental results were based on the average value of three parallel tests. The initial data of the experiment was collected by HPLC, and the original 9.0 software was used to process the data.

### Results and Discussion

#### Effect of Temperature on the Degradation of ATZ over UV/PMS

In PB with pH value of 7, the influence of different temperatures on the degradation of ATZ by UV/PMS was shown in Fig. 1 when the ATZ concentration, UV intensity and PMS concentration were, respectively, 2.5 μmol/L, 50 mW/cm<sup>2</sup> and 20 μmol/L. According to Fig. 1, with the increase of reaction temperature, the effect of degradation of ATZ by UV/PMS is increasing. The removal rate of ATZ increased from 59.56% to 80.32%, when the temperature of the reaction system increased from 10°C to 25°C. The removal rate of ATZ when the temperature increased from 15°C to 20°C was greater than those from 10°C to 15°C, and from 20°C to 25°C, indicating that temperature has less influence on ATZ degradation in normal temperature.

#### The Effect of PMS Concentration on the Degradation of ATZ by UV/PMS

In PB with pH value of 7 under 20°C, the influence of different PMS concentrations on the degradation of ATZ by UV/PMS is shown in Fig. 2, when the ATZ concentration and UV intensity were, respectively, 2.5 μmol/L and 50mW/cm<sup>2</sup>. According to Fig. 2, with the increase of PMS concentration, the effect of degradation

of ATZ by UV/PMS is increasing. The removal rate of ATZ increased from 59.04% to 97.63%, when the PMS concentration of the reaction system increased from 10 μmol/L to 50 μmol/L. The removal rate of ATZ when the PMS concentration increased from 10 μmol/L to 30 μmol/L was greater than those from 30 μmol/L to 50 μmol/L, indicating that PMS concentration has great influence on the degradation of ATZ by UV/PMS.

#### Effect of pH Value on the Degradation of ATZ by UV/PMS

In PB with different pH values under 20°C, the influence of different pH values on the degradation of ATZ by UV/PMS is shown in Fig. 3 when the ATZ concentration, UV intensity and PMS concentration were, respectively, 2.5 μmol/L, 50 mW/cm<sup>2</sup> and 20 μmol/L. According to Fig. 3, with the increase of pH value in the reaction system, the effect of degradation of ATZ by UV/PMS is increasing. The removal rates

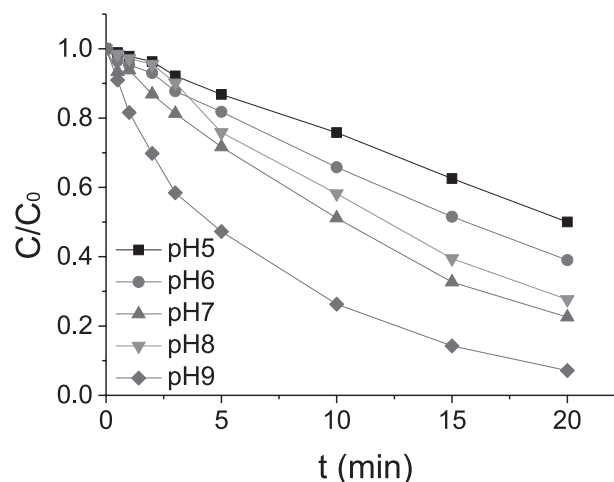
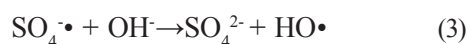
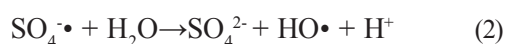
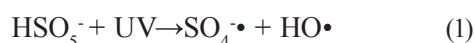


Fig. 3. ATZ removal rates under different pH values.

of ATZ were respectively 49.98%, 60.98%, 77.40%, 72.35% and 92.87% when the pH of the reaction system were 5, 6, 7, 8 and 9, respectively. Notably, the removal rate of ATZ increased from 60.98% to 77.40% when the pH value of the reaction system increased from 6 to 7, while the removal rate decreased from 77.40% to 72.35% when the pH value of the reaction system increased from 7 to 8. The removal rate of ATZ under alkaline conditions is higher than that in acidic conditions, with the main reasons as follows: UV could excite PMS to generate  $\text{SO}_4^{\cdot-}$  and  $\text{HO}\cdot$  (the equation is shown in 1-1) and  $\text{HO}\cdot$  has slightly more oxidizing capacity to ATZ than  $\text{SO}_4^{\cdot-}$ , the secondary reaction rates of  $\text{SO}_4^{\cdot-}$  and  $\text{HO}\cdot$  are  $3\times 10^9 \text{ M}^{-1}\text{s}^{-1}$ [18] and  $2.59\times 10^9 \text{ M}^{-1}\text{s}^{-1}$ [19]. The  $\text{SO}_4^{\cdot-}$  could react with water in aqueous conditions of various pH value to produce  $\text{HO}\cdot$  with the reaction rate constant of  $8.30 \text{ M}^{-1}\text{s}^{-1}$  [20] (the equation is shown in equations 1-2), while in alkaline conditions,  $\text{SO}_4^{\cdot-}$  could also react with  $\text{OH}^-$  to produce  $\text{HO}\cdot$ , and its reaction rate constant was  $6.50\times 10^7 \text{ M}^{-1}\text{s}^{-1}$  [21] (the equation is shown in equations 1-3). The pH value changes generally did not affect the yield of  $\text{SO}_4^{\cdot-}$  in UV/PMS. Therefore, more  $\text{HO}\cdot$  was produced in the UV/PMS system under alkaline conditions, so the removal rate of ATZ under alkaline conditions was higher than that under acidic conditions. The removal rate of ATZ under pH 8 was slightly lower than that under pH 7, mainly because there were different forms of phosphate in the buffer solution. The  $\text{H}_2\text{PO}_4^-$  ionized in aqueous solution (the equation is shown in equations 1-4), with the ionization constant of  $K$  reaching  $6.31\times 10^{-8}$ , so equation 1-5 could be figured out. According to equation 1-5, as the pH of the solution increased, the amount of  $\text{HPO}_4^{2-}$  in the solution gradually increased and the amount of  $\text{H}_2\text{PO}_4^-$  decreased gradually. The reaction rates of  $\text{HPO}_4^{2-}$  with  $\text{SO}_4^{\cdot-}$  and  $\text{HO}\cdot$  were, respectively,  $1.20\times 10^6 \text{ M}^{-1}\text{s}^{-1}$  and  $1.50\times 10^5 \text{ M}^{-1}\text{s}^{-1}$ , while the reaction rates of  $\text{H}_2\text{PO}_4^-$  with  $\text{SO}_4^{\cdot-}$  and  $\text{HO}\cdot$  were, respectively,  $7.20\times 10^4 \text{ M}^{-1}\text{s}^{-1}$  and  $2.00\times 10^4 \text{ M}^{-1}\text{s}^{-1}$  [20]. Therefore, the amount of  $\text{HPO}_4^{2-}$  increased gradually when the pH value of the solution increased, and it competed with the target object ATZ for  $\text{SO}_4^{\cdot-}$  and  $\text{HO}\cdot$ , which resulted in the decrease of ATZ degradation efficiency. The degradation efficiency of ATZ in pH 9 is significantly higher than that of pH7 and pH8, mainly because  $\text{SO}_4^{\cdot-}$  was very easy to react with  $\text{OH}^-$  to form  $\text{HO}\cdot$ , which makes the system contain a large number of  $\text{HO}\cdot$  in a short time, thus accelerating the degradation of ATZ.



$$\text{pH} = 7.20 + \text{Lg}([\text{HPO}_4^{2-}]/[\text{H}_2\text{PO}_4^-]) \quad (5)$$

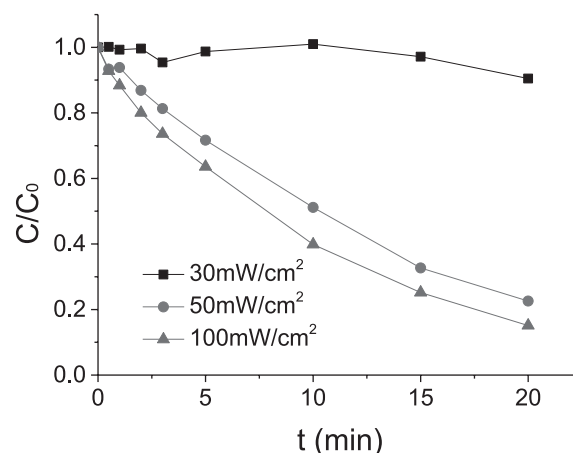


Fig. 4. ATZ removal rates under different UV intensities.

### Effect of UV Intensity on the Degradation of ATZ by UV/PMS

In PB with pH value of 7 under 20°C, the influence of different UV intensities on the degradation of ATZ by UV/PMS is shown in Fig. 4, when the concentrations of ATZ and PMS were, respectively, 2.5  $\mu\text{mol/L}$  and 20  $\mu\text{mol/L}$ . According to Fig. 4, with the increase of UV intensity in the reaction system, the effect of ATZ degradation by UV/PMS was increased rapidly. The removal rate of ATZ increased from 9.51% to 84.89% when the UV intensity increased from 30  $\text{mW/cm}^2$  to 100  $\text{mW/cm}^2$ . The removal rate of ATZ when the UV intensity increased from 30  $\text{mW/cm}^2$  to 50  $\text{mW/cm}^2$  was greater than those from 50  $\text{mW/cm}^2$  to 100  $\text{mW/cm}^2$ , indicating that UV intensity had great influence on the degradation of ATZ by UV/PMS.

### Effect of ATZ Concentration on the Degradation of ATZ by UV/PMS

In PB with pH value of 7 under 20°C, the influence of different ATZ concentrations on the degradation

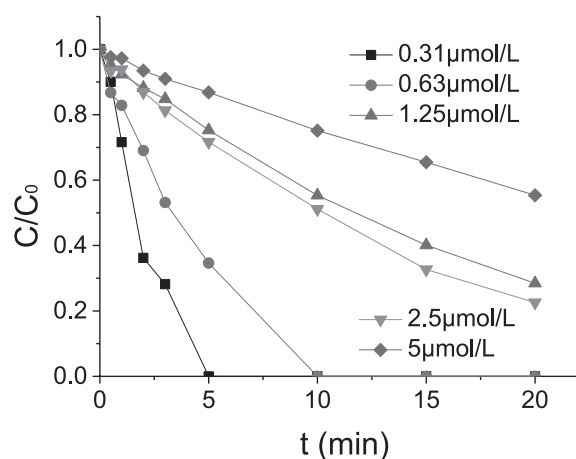


Fig. 5. ATZ removal rates under different ATZ densities.

of ATZ by UV/PMS is shown in Fig. 5 when the UV intensity and PMS concentration were, respectively, 50 mW/cm<sup>2</sup> and 20 μmol/L. According to Fig. 5, with the increase of ATZ concentration in the reaction system, the effect of ATZ degradation by UV/PMS was gradually weakened. The removal rate of ATZ dropped from 100% to 44.64% when ATZ concentration increased from 0.31 μmol/L to 5 μmol/L, the removal rate of ATZ decreased from 77.40% to 44.64% when the ATZ concentration increased from 2.5 μmol/L to 5 μmol/L. The removal rate of ATZ slightly increased from 71.55% to 77.40% when the concentration of ATZ increased from 1.25 μmol/L to 2.5 μmol/L. This is mainly caused by the following two reasons. One is in the case of other conditions unchanged, with the decrease of the ATZ concentration in the reaction system, collisions between single molecules with SO<sub>4</sub>•<sup>-</sup> and HO• were less in unit time, therefore the ability of ATZ to capture SO<sub>4</sub>•<sup>-</sup> and HO• in the reaction system was reduced. Second, the second-order reaction rate of HSO<sub>5</sub><sup>-</sup> with SO<sub>4</sub>•<sup>-</sup> and HO• were 1.0×10<sup>6</sup> M<sup>-1</sup>s<sup>-1</sup> and 1.0×10<sup>7</sup> M<sup>-1</sup>s<sup>-1</sup>, resulting in the capture of some SO<sub>4</sub>•<sup>-</sup> and HO• by HSO<sub>5</sub><sup>-</sup>. The research of Sharma et al. [22] showed that in the process of bisphenol A (BPA) degradation by UV-C/PMS, the removal rate of BPA was reduced when the initial concentration of BPA was less than 0.13 mM. Similar experimental phenomenon was observed in this experiment. Moreover, as the concentration of ATZ continues to decrease (0.31 μmol/L, 0.63 μmol/L), even if SO<sub>4</sub>•<sup>-</sup> and HO• are caught by HSO<sub>5</sub><sup>-</sup>, the concentration of SO<sub>4</sub>•<sup>-</sup> and HO• in the UV/PMS system is too high compared with that of ATZ, so the degradation rate of ATZ can reach 100%. Given the above, the effect of ATZ concentration has great influence on the degradation of ATZ by UV/PMS.

#### Degradation Mechanism Analysis of ATZ by UV/PMS

The degradation mechanism of ATZ by UV/PMS was analyzed by a single-factor method in PB with the concentration of 1.25 mmol/L and pH value of 7 when the UV intensity, PMS concentration, temperature and ATZ concentration were 50 mW/cm<sup>2</sup>, 20 μmol/L, 20°C and 2.5 μmol/L, respectively (Fig. 6).

According to Fig. 6a), PB alone had no degrading effect on ATZ, and single PB at the present concentration only weakly degraded ATZ. The degradation efficiency of single UV to ATZ was 37.56%, accounting for 48.51% of the total removal rate. The degradation efficiency of UV/PB to ATZ was 50.97%, showing a 13.41% degradation efficiency increase compared with single UV. The main reasons are as follows: in PB solution with pH value of 7, phosphate mainly existed in the form of HPO<sub>4</sub><sup>2-</sup> and H<sub>2</sub>PO<sub>4</sub><sup>-</sup> with their quantity ratio close to 1:1, and UV could stimulate the generation of HPO<sub>4</sub>•<sup>-</sup> and H<sub>2</sub>PO<sub>4</sub>• with certain oxidative properties to ATZ. For another, PB could excite PMS to generate

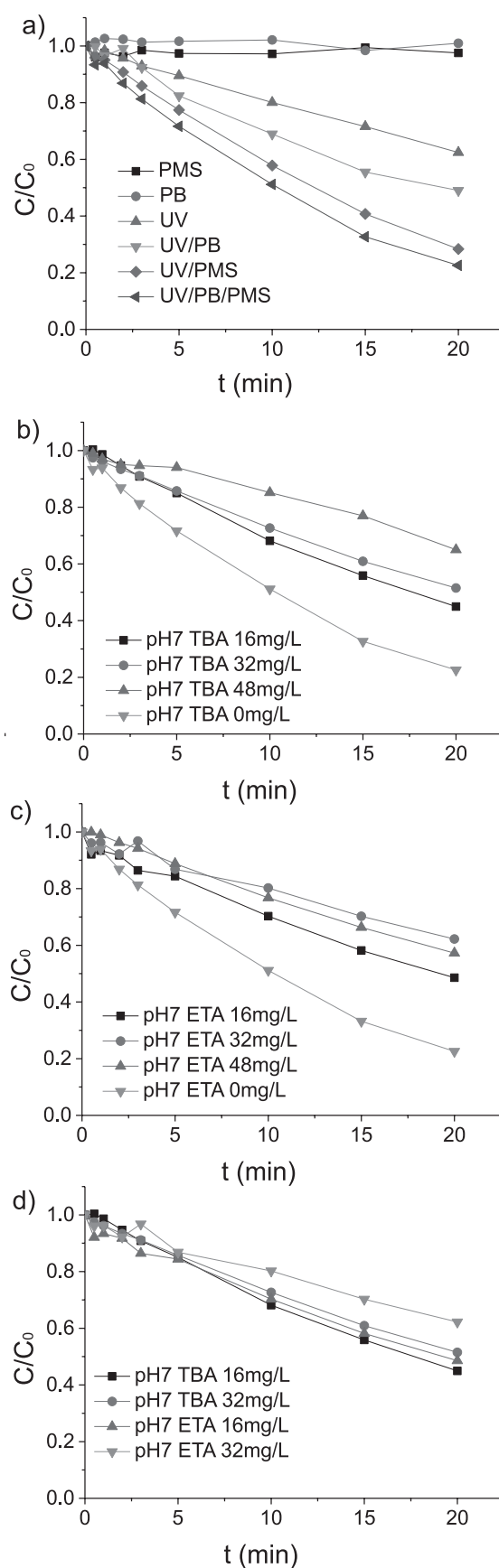


Fig. 6. a) Analysis of oxidation effect of each component in the UV/PMS system, b) effect of TBA on the degradation of ATZ by UV/PMS in pH7 PB, c) effect of ETA on the degradation of ATZ by UV/PMS in pH7 PB, and d) comparison of TBA and ETA on UV/PMS degradation ATZ in pH 7 PB.

$\text{SO}_4\cdot^-$  and  $\text{HO}\cdot$  [23], so the degradation efficiency of UV/PB to ATZ was slightly higher than that of single UV. The degradation efficiency of UV/PMS to ATZ was 71.64%, showing a 20.67% increase compared with those of UV/PB. This is mainly because UV could excite PMS to generate  $\text{SO}_4\cdot^-$  and  $\text{HO}\cdot$ , whose degradation efficiency to ATZ was higher than those of  $\text{HPO}_4\cdot^-$  and  $\text{H}_2\text{PO}_4\cdot^-$ , so the degradation efficiency of UV/PMS to ATZ was higher than those of single UV/PB. The degradation efficiency of UV/PB/PMS (only here differentiate between the UV/PB/PMS system and UV/PMS system, the rest of the UV/PMS system indicates in PB) to ATZ was slightly higher than those of UV/PMS. This is mainly because the initial pH of the UV/PMS reaction system was set to 7 by NaOH. After the reaction, the whole system became acidic, and the pH value of the UV/PB/PMS system was stable to 7. The experimental conditions were similar to the above situations under the circumstances of acid pH value and alkaline pH value, and specific analysis is not elaborated upon here. According to the study of Dionysiou et al. [24], the reaction rate of TBA with  $\text{HO}\cdot$  and  $\text{SO}_4\cdot^-$  were respectively  $3.8\text{--}7.6\times 10^8 \text{ M}^{-1}\text{s}^{-1}$  and  $4\text{--}9.1\times 10^5 \text{ M}^{-1}\text{s}^{-1}$ , while the research of Buxton et al. [25] showed that the reaction rates of ETA with  $\text{HO}\cdot$  and  $\text{SO}_4\cdot^-$  were respectively  $1.2\text{--}2.8\times 10^9 \text{ M}^{-1}\text{s}^{-1}$  and  $1.6\text{--}7.7\times 10^7 \text{ M}^{-1}\text{s}^{-1}$ . Therefore, When  $\text{HO}\cdot$  and  $\text{SO}_4\cdot^-$  coexist in the reaction system,  $\text{HO}\cdot$  can be captured by TBA while  $\text{HO}\cdot$  and  $\text{SO}_4\cdot^-$  are captured by ETA. According to Fig. 6(b-c), the addition of TBA and ETA could effectively inhibit the degradation of ATZ by UV/PMS, and the inhibition effect of ETA was stronger than TBA. As shown in Fig. 6d),  $\text{HO}\cdot$  and  $\text{SO}_4\cdot^-$  coexist in the UV/PMS system.

#### Effect of Common Anions Concentration in Waters on the Degradation of ATZ by UV/PMS

In PB with pH value of 7 and concentration of 1.25 mmol/L under 20°C, the influence of common anions in waters as  $\text{Cl}^-$ ,  $\text{HCO}_3^-$  and  $\text{NO}_3^-$  on the degradation of ATZ by UV/PMS was shown in Fig. 7 when UV intensity, PMS concentration and ATZ concentration were respectively 50 mW/cm<sup>2</sup>, 20 μmol/L and 2.5 μmol/L. According to Fig. 7,  $\text{Cl}^-$  and  $\text{HCO}_3^-$  both had inhibitory effects on the degradation of ATZ in the system at the same concentration, mainly because  $\text{Cl}^-$  and  $\text{HCO}_3^-$  could compete with ATZ for  $\text{HO}\cdot$  and  $\text{SO}_4\cdot^-$  in the UV/PMS system to generate  $\text{Cl}_2\cdot^-$ ,  $\text{ClOH}\cdot$  and  $\text{CO}_3\cdot^-$ , whose reaction rates were lower than those of  $\text{HO}\cdot$  and  $\text{SO}_4\cdot^-$ . It is easy to observe that the inhibiting effect of  $\text{Cl}^-$  was higher than  $\text{HCO}_3^-$ , and specific performances were as follows: the degradation efficiency of ATZ was reduced from 77.40% to 41.14% and 63.58% respectively after adding 2 mmol/L of  $\text{Cl}^-$  and  $\text{HCO}_3^-$  to the UV/PMS system. This is mainly because the secondary reaction constants of  $\text{Cl}_2\cdot^-$  and ATZ were lower than those of  $\text{CO}_3\cdot^-$  and ATZ (the main equation is shown in formula 1-6 to 1-13).

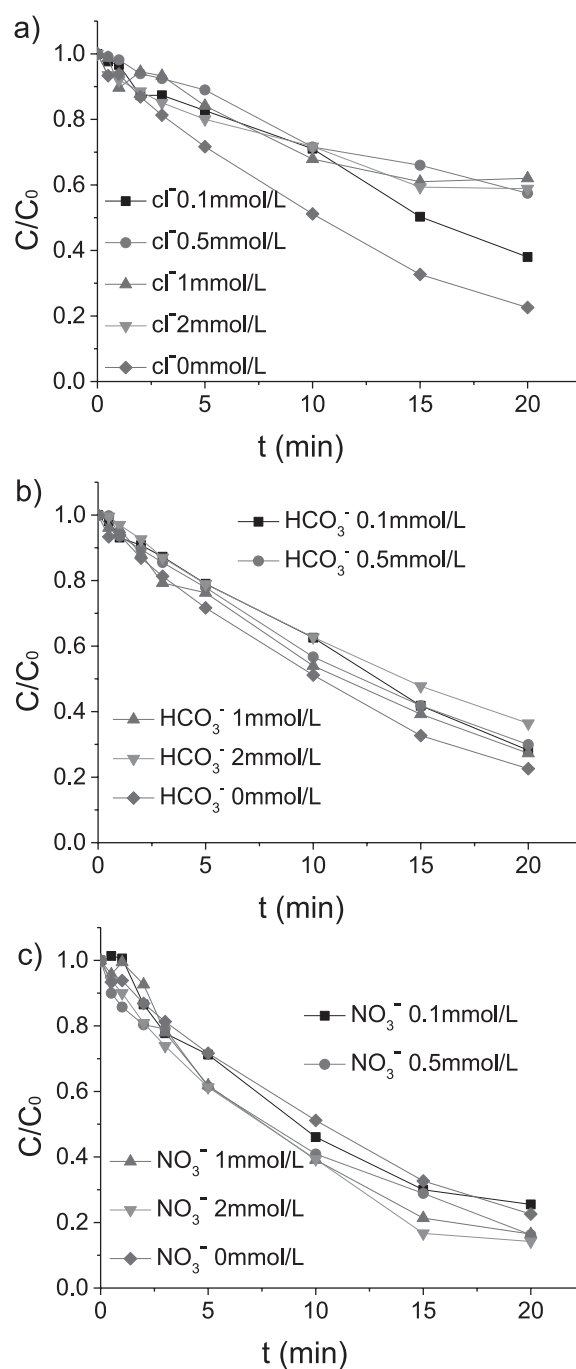
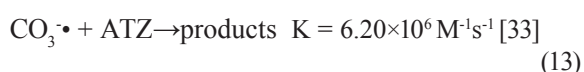
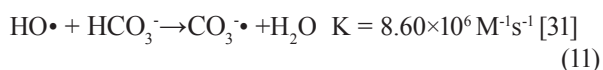
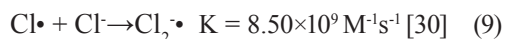
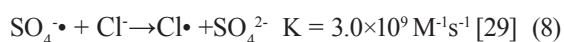
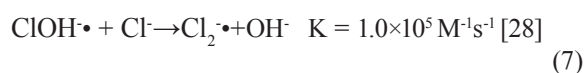
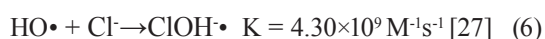


Fig. 7. a) Effect of  $\text{Cl}^-$  on the degradation of ATZ by UV/PMS in pH7 PB, b) effect of  $\text{HCO}_3^-$  on the degradation of ATZ by UV/PMS in pH7 PB, and c) effect of  $\text{NO}_3^-$  on degradation of ATZ by UV/PMS in pH 7 PB.

While  $\text{NO}_3^-$  showed a positive effect on the degradation of ATZ in the UV/PMS system at same concentration, specifically the degradation efficiency of ATZ increased from 77.40% to 85.81 when  $\text{NO}_3^-$  of 2 mmol/L was added to the UV/PMS system. This is mainly because UV could excite  $\text{NO}_3^-$  to generate  $\text{HO}\cdot$ ,  $\text{NO}_2\cdot^-$  and  $\text{NO}_2$  free radical, etc. [26]. Therefore, the steady state concentration of  $\text{HO}\cdot$  in the UV/PMS system was improved, and the efficiency of ATZ degradation by UV/PMS was accelerated.



### Kinetic Analysis of ATZ Degradation by UV/PMS

According to the study of Simonin et al. [34] the kinetic model of ATZ degradation by  $\text{O}_3$  oxidation was established according to the following dynamic equations, and the first-order reaction kinetics equation is as follows:

$$\ln(c/c_0) = -K_1 t \quad (14)$$

The second-order reaction kinetic equation is as follows:

$$1/c = K_2 t + 1/c_0 \quad (15)$$

Substitute the condition of  $c/c_0 = 1 - \gamma$  into equation 1-2, and the attainable equation is as follows:

$$1/(1-\gamma) = K_2 c_0 t + 1 \quad (16)$$

$c$ : ATZ concentration in any time,  $\mu\text{mol/L}$

$c_0$ : ATZ concentration on the moment of 0,  $\mu\text{mol/L}$

$\gamma$ : Removal rate of ATZ

$K_1$ : Pseudo first-order reaction rate constant,  $\text{min}^{-1}$

$K_2$ : Pseudo secondary reaction rate constant,  $(\mu\text{mol/L})^{-1}\text{min}^{-1}$

In PB with the concentration of 1.25 mmol/L and pH 7, the reaction of ATZ degradation by UV/PMS was simulated by first-order reaction kinetics under the following conditions: UV intensity, PMS concentration, temperature and ATZ concentration were 50 mW/cm<sup>2</sup>, 20  $\mu\text{mol/L}$ , 20°C and 2.5  $\mu\text{mol/L}$ , respectively; concentrations of  $\text{Cl}^-$ ,  $\text{HCO}_3^-$ ,  $\text{NO}_3^-$  and ETA were all 1 mmol/L; the X-axis was set by  $t(x)$  and Y-axis was set by  $\ln(C/C_0)$ . The reaction of ATZ degradation by UV/PMS was simulated by Quasi second-order reaction kinetics fitting, by  $t(x)$  as X-axis

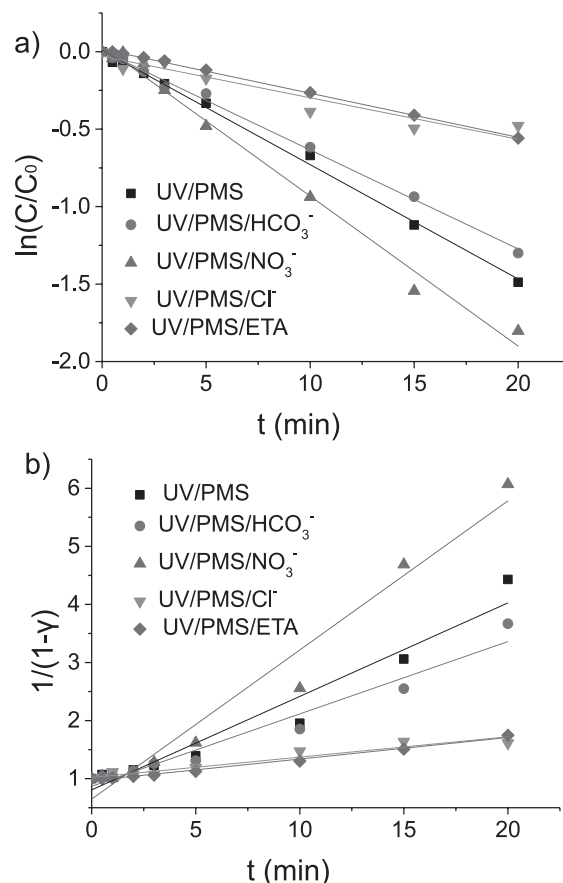


Fig. 8. a) Kinetics of quasi first-order reaction of UV/PMS degradation ATZ and b) kinetics of quasi second-order reaction of UV/PMS degradation ATZ.

and  $1/(1-\gamma)(y)$  as Y-axis. The dynamic fitting curve is shown in Fig. 8, and the dynamic fitting parameters are shown in Table 2. According to Fig. 8 and Table 2, the  $R^2$  value (linear correlation) of the quasi first-order reaction kinetics is larger than the  $R^2$  value of the quasi second-order reaction kinetics (except the UV/PMS/ $\text{Cl}^-$  system), indicating that the reaction of ATZ degradation by UV/PMS was more consistent with the quasi first-order reaction kinetics. ETA and  $\text{Cl}^-$  of the same concentration have the same inhibitory effect on the degradation of ATZ by UV/PMS. Both of them reduced the rate of ATZ degradation to 38.54% and 36.29% respectively, and the addition of  $\text{NO}_3^-$  improved the rate of ATZ degradation by 31.21% on an original basis.

### Analysis of Degradation Product of ATZ by UV/PMS and its Degradation Path

The degradation products of ATZ by UV/PMS were analyzed by HPLC-ESI-MS(cationic mode), and the degradation path was speculated. The three samples were extracted from 3, 10 and 20 min in the process of the experiment, then conducted the first-order mass spectrum scanning, and the total ions and extracted ions were analyzed. According to the mass spectrum,

Table 2. Kinetic parameters of UV/PMS degradation of ATZ.

Reaction System	Reaction Rate Constant		R <sup>2</sup>	
	First-Order Reaction (min <sup>-1</sup> )	Second-Order Reaction (μmol/L) <sup>-1</sup> min <sup>-1</sup>	First-Order Reaction	Second-Order Reaction
UV/PMS	-0.07383	0.16097	0.99652	0.94529
UV/PMS/HCO <sub>3</sub> <sup>-</sup>	-0.06391	0.12451	0.99611	0.95446
UV/PMS/NO <sub>3</sub> <sup>-</sup>	-0.09687	0.25677	0.98854	0.96390
UV/PMS/Cl <sup>-</sup>	-0.02679	0.03501	0.90457	0.91618
UV/PMS/ETA	-0.02845	0.03716	0.99840	0.98942

total ion chromatogram and extracted ion flow diagrams from the three samples extracted at 3, 10 and 20min, the mass-to-charge ratio of the main degradation products of ATZ was 174, 188, 198, 214, 232, etc. The relative molecular weight of ATZ is 216, m/z174 has a molecular weight 42 less than ATZ, which is the molecular weight of isopropyl, thus m/z174 is regarded as deisopropyl ATZ, that is 2-chloro-4-diethylamino-6-amino atrazin, CDAA; m/z188 has a molecular weight 28 less than ATZ, which is the molecular weight of ethyl, thus m/z188 is regarded as desetylatrazine ATZ, namely 2-chloro-4-amino-6-isopropylamino atrazine, CAIA. m/z198 has a molecular weight 18 less than ATZ, thus it is believed that in the process of ATZ degradation, Cl atoms are replaced by hydroxyl groups to produce 2-hydroxy-4-diethylamino-6-isopropylamino atrazine, HDIA. m/z232 has a molecular weight 16 greater than ATZ, which is the molecular weight of hydroxy, thus consider in the process of ATZ degradation, a hydrogen atom was replaced by a hydroxyl group to produce 2-Chloro-4-hydroxyethylamino-6-isopropyl atrazine, CHIA. m/z214 has a molecular weight 18 less than

CHIA, thus m/z214 is regarded as the dehydration products of CHIA, namely 2-Chloro-4-vinylamino-6-isopropyl atrazine (214), CVIA. And m/z214 has a molecular weight 16 greater than HDIA, thus m/z214 is regarded as the product of the substitution of a hydrogen atom in HDIA replaced by hydroxyl group, that is 2-hydroxy-4-hydroxyethylamino-6-isopropyl atrazine, HHIA. Khan et al.[19] showed the similar results. The degradation path of ATZ is shown in Fig. 9.

## Conclusions

The higher the temperature in normal range (10-25°C), the higher the degradation efficiency of UV/PMS to ATZ, but the temperature change in normal range has little effect on the efficiency of the ATZ degradation by UV/PMS. The degradation efficiency of UV/PMS to ATZ improved as the concentration of PMS and UV intensity increased. The changes of ATZ concentration and pH values are not positively correlated with the degradation efficiency of ATZ by UV/PMS.

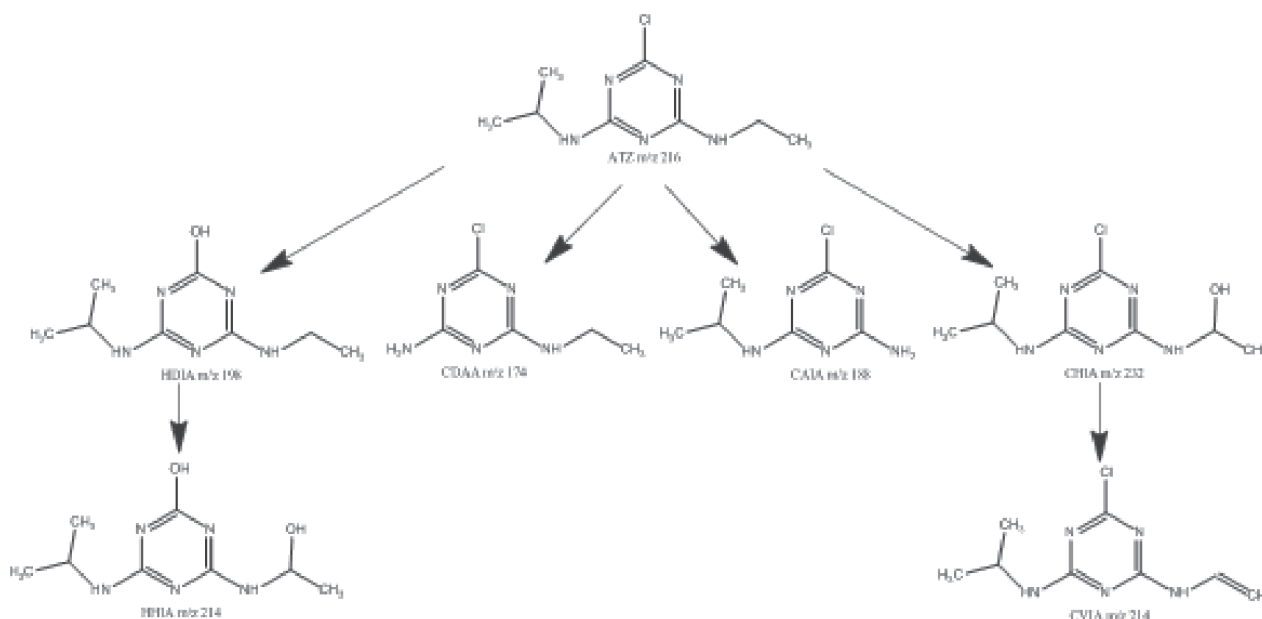


Fig. 9. Degradation pathway of ATZ.



The PB in alkaline conditions are more conducive to the degradation of ATZ by UV/PMS than the PB under acidic conditions. PB under alkaline conditions has a complex influence on the degradation of ATZ by UV/PMS, and the reaction is closely related to the state of phosphate, and generally no positive correlation. HO• and SO<sub>4</sub>• coexist in the UV/PMS system, and the degradation quantity ratio of ATZ by UV reacted with HO• and SO<sub>4</sub>• approached 1:1. Both Cl<sup>-</sup> and HCO<sub>3</sub><sup>-</sup> showed suppressive effects on the degradation of ATZ by the UV/PMS system, and the inhibiting effect of Cl<sup>-</sup> is more obvious, while NO<sub>3</sub><sup>-</sup> has a catalytic effect on the degradation of ATZ by the UV/PMS system. The reaction kinetics of ATZ degradation by UV/PMS is more consistent with Quasi first-order reaction kinetics. By LC-MS analysis, 5 kinds of production m/z and 6 kinds of products were obtained.

### Acknowledgements

This study was financially supported by the Key Project of Education Department in Sichuan Province under grant No. 17ZB0031; the Science and Technology Project of Sichuan Province under grant No. 2017GZ0375; and the Technology Research and Development Project of Chengdu under grant No. 2015-HM01-00333-SF.

### Conflict of Interest

The authors declare no conflict of interest.

### References

1. BARCHANSKA H., SAJDAK M., SZCZYPKA K., SWIENTEK A., TWOREK M., KUREK M. Atrazine, triketone herbicides, and their degradation products in sediment, soil and surface water samples in poland. *Environmental Science & Pollution Research*, **24** (1), 644, **2017**.
2. GAO J., SONG P., WANG G., WANG J., ZHU L., WANG J. Responses of atrazine degradation and native bacterial community in soil to *Arthrobacter* sp. strain HB-5. *Ecotoxicology and Environmental Safety*, **159**, 317, **2018**.
3. BO'DALO A., LEO'N G., HIDALGO A.M., GO'MEZ M., MURCIA M.D., BLANCO P. Atrazine removal from aqueous solutions by nanofiltration. *Desalination & Water Treatment*, **13** (1-3), 143, **2010**.
4. POTTER T.L., BOSCH D.D., DIEPPA A., WHITALL D.R., STRICKLAND T.C. Atrazine fate and transport within the coastal zone in southeastern puerto rico. *Marine Pollution Bulletin*, **67** (1-2), 36, **2013**.
5. MESSING P., FARENHORST A., WAITE D., SPROULL J. Influence of usage and chemical-physical properties on the atmospheric transport and deposition of pesticides to agricultural regions of Manitoba, Canada. *Chemosphere*, **90** (6), 1997, **2012**.
6. KOMSKY-ELBAZ A., ROTH Z. Effect of the herbicide atrazine and its metabolite DACT on bovine sperm quality. *Reproductive Toxicology*, **67**, 15, **2016**.
7. OLIVEIRA H.C., STOLF-MOREIRA R., MARTINEZ C.B.R., GRILLO R., JESUS M. B.D., FRACETO L.F. Nanoencapsulation enhances the post-emergence herbicidal activity of atrazine against mustard plants. *Plos One*, **10** (7), e0132971, **2015**.
8. KURTKARAKUS P.B., MUIR D.C.G., BIDLEMAN T.F., SMALL J., BACKUS S., DOVE A. Metolachlor and atrazine in the great lakes. *Environmental Science & Technology*, **44** (12), 4678, **2010**.
9. SOLOMON K.R., GIESY J.P., LAPOINT T.W., GIDDINGS J.M., RICHARDS R.P. Ecological risk assessment of atrazine in north american surface waters. *Environmental Toxicology & Chemistry*, **32** (1), 10, **2013**.
10. NWANI C.D., LAKRA W.S., NAGPURE N.S., KUMAR R., KUSHWAHA B., SRIVASTAVA S.K. Toxicity of the herbicide atrazine: effects on lipid peroxidation and activities of antioxidant enzymes in the freshwater fish channa punctatus (bloch). *International Journal of Environmental Research & Public Health*, **7** (8), 3298, **2010**.
11. TAVERAMENDOZA L., RUBY S., BROUSSEAU P., FOURNIER M., CYR D., MARCOGLIESE D. Response of the amphibian tadpole xenopus laevis to atrazine during sexual differentiation of the ovary. *Environmental Toxicology & Chemistry*, **21** (6), 1264, **2002**.
12. HAYES T., HASTON K., TSUI M., HOANG A., HAEFFELE C., VONK A. Atrazine-induced hermaphroditism at 0.1 ppb in american leopard frogs (*rana pipiens*): laboratory and field evidence. *Environmental Health Perspect*, **111** (4), 568, **2003**.
13. HAYES T., HASTON K., TSUI M., HOANG A., HAEFFELE C., VONK A. Herbicides: feminization of male frogs in the wild. *Nature*, **419** (6910), 895, **2002**.
14. RINSKY J.L., HOPENHAYN C., GOLLA V., BROWNING S., BUSH H.M. Atrazine exposure in public drinking water and preterm birth. *Public Health Reports*, **127** (1), 72, **2012**.
15. JI Y., DONG C., KONG D., LU J., ZHOU Q. Heat-activated persulfate oxidation of atrazine: implications for remediation of groundwater contaminated by herbicides. *Chemical Engineering Journal*, **263**, 45, **2015**.
16. JI Y., DONG C., KONG D., LU J. New insights into atrazine degradation by cobalt catalyzed peroxymonosulfate oxidation: kinetics, reaction products and transformation mechanisms. *Journal of Hazardous Materials*, **285**, 491, **2015**.
17. BU L., SHI Z., ZHOU S. Modeling of fe(ii)-activated persulfate oxidation using atrazine as a target contaminant. *Separation & Purification Technology*, **169**, 59, **2016**.
18. LUTZE H. V., BIRCHER S., RAPP I., KERLIN N., BAKKOUR R., GEISLER M., et al. Degradation of chlorotriazine pesticides by sulfate radicals and the influence of organic matter. *Environmental Science & Technology*, **49** (3), 1673, **2015**.
19. KHAN J.A., HE X., SHAH N.S., KHAN H.M., HAPESHI E., FATTA-KASSINOS D., et al. Kinetic and mechanism investigation on the photochemical degradation of atrazine with activated H<sub>2</sub>O<sub>2</sub>, S<sub>2</sub>O<sub>8</sub><sup>2-</sup>, and HSO<sub>5</sub><sup>-</sup>. *Chemical Engineering Journal*, **252** (18), 393, **2014**.
20. LUO C., MA J., JIANG J., LIU Y., SONG Y., YANG Y., et al. Simulation and comparative study on the oxidation

- kinetics of atrazine by UV/H<sub>2</sub>O<sub>2</sub>, UV = HSO<sub>5</sub><sup>-</sup> and UV = S<sub>2</sub>O<sub>8</sub><sup>2-</sup>. *Water Research*, **80**, 99, **2015**.
21. HAYON E., TREININ A., WILF J. Electronic spectra, photochemistry, and autoxidation mechanism of the sulfite-bisulfite-pyrosulfite systems. The SO<sub>2</sub><sup>-</sup>, SO<sub>3</sub><sup>-</sup>, SO<sub>4</sub><sup>-</sup>, and SO<sub>5</sub><sup>-</sup> radicals. *Journal of the American Chemical Society*, **94**, 47, **1972**.
  22. SHARMA J., MISHRA I. M., DIONYSIOU D. D., KUMAR V. Oxidative removal of bisphenol a by UV-C/peroxymonosulfate (pms): kinetics, influence of co-existing chemicals and degradation pathway. *Chemical Engineering Journal*, **276**, 193, **2015**.
  23. LOU X., WU L., GUO Y., CHEN C., WANG Z., XIAO D., et al. Peroxymonosulfate activation by phosphate anion for organics degradation in water. *Chemosphere*, **117** (117), 582, **2014**.
  24. DIONYSIOU D., ANIPSITAKIS G. P. Radical generation by the interaction of transition metals with common oxidants. *Environmental Science & Technology*, **38**, 3705, **2004**.
  25. BUXTON G.V., GREENSTOCK C.L., HELMAN W.P., ROSS A.B. Critical review of rate constants for reactions of hydrated electrons, hydrogen atoms and hydroxyl radicals (HO•/•O-) in aqueous solution. *The Journal of Chemical Physics*, **17**, 513, **1988**.
  26. SHAH A.D., MITCH W.A. Halonitroalkanes, halonitriles, haloamides, and N-nitrosamines: A critical review of N-nitrogenous disinfection by product formation pathways. *Environmental Science & Technology*, **46** (1), 119, **2011**.
  27. ZHU H., WANG Q., NI J., TONG S. Effect of different common anions on oxidative efficiency of TiO<sub>2</sub>/H<sub>2</sub>O<sub>2</sub>/O<sub>3</sub>. *Chinese Journal of Environmental Engineering*, **10** (8), 4172, **2016** [In Chinese].
  28. MINAKATA D., KAMATH D., MAETZOLD S. Mechanistic insight into the reactivity of chlorine-derived radicals in the aqueous-phase uv/chlorine advanced oxidation process: quantum mechanical calculations. *Environmental Science & Technology*, **51** (12), 6918, **2017**.
  29. DAS T.N. Reactivity and role of SO<sub>5</sub><sup>•</sup> radical in aqueous medium chain oxidation of sulfite to sulfate and atmospheric sulfuric acid generation. *Journal of Physical Chemistry A*, **105** (40), 9142, **2001**.
  30. WANG P., YANG S., NIU R., SHAO X. Involvements of chloride ion in decolorization of Acid Orange 7 by activated peroxydisulfate or peroxymonosulfate oxidation. *Journal of Environmental Sciences*, **23** (11), 1799, **2011**.
  31. LUO C., JIANG J., MA J., PANG S., LIU Y., SONG Y., GUAN C., LI J., JIN Y., WU D. Oxidation of the odorous compound 2,4,6-trichloroanisole by uv activated persulfate: kinetics, products, and pathways. *Water Research*, **96**, 12, **2016**.
  32. XIE X., ZHANG Y., HUANG W., HUANG S. Degradation kinetics and mechanism of aniline by heat-assisted persulfate oxidation. *Journal of Environmental Sciences*, **24** (5), 821, **2012**.
  33. HUANG J., MABURY S.A. A new method for measuring carbonate radical reactivity toward pesticides. *environmental toxicology and chemistry*, **19** (6), 1501, **2000**.
  34. SIMONIN J.P. On the comparison of pseudo-first order and pseudo-second order rate laws in the modeling of adsorption kinetics. *Chemical Engineering Journal*, **300**, 254, **2016**.